

Mathematical Tutorial of Discrete-Time Analysis of Aliasing and Non-Aliasing Periodic Sampling Concept with Fourier Analysis for Digital Signal Processing and Digital Communication Prospective**

Vorapoj Patanavijit* & Kornkamol Thakulsukanant
Assumption University of Thailand

วรพจน์ พัฒนวิจิตร* และกรกมล ตระกูลสุขอนันต์
มหาวิทยาลัยอัสสัมชัญ

Abstract

Due to a large requirement of both digital signals (which are the digitized Discrete-Time (DT) signals) and Discrete-Time (DT) signals (such as speech, image, data, etc.) for implementation and research of the modern algorithms and mathematical techniques for application in modern electronic devices based on microprocessors/microcontrollers (such as smart phone, PDA and digital camera, etc.), the real observed signals, which usually are Continuous-Time (CT) signals, can be converted into Discrete-Time (DT) signals by using any mathematical sampling techniques: a uniform sampling with various parametric basis expansion modeling or a non-uniform sampling. Consequently, this paper presents the mathematical tutorial of Discrete-Time (DT) analysis of aliasing and non-aliasing sampling concepts for periodic signals in the frequency domain. First, this paper mathematically presents the periodic sampling concept and, later, reviews the frequency domain mathematical analysis in the sampling system/result, the reconstruction/result and the Nyquist-Shannon sampling theorem. Finally, an example of a sampling process and a reconstruction process, which are explained in each mathematical detail, are given in order to help the reader deeply and clearly understand.

Keywords: Continuous-Time Fourier Transform (CT-FT), Discrete-Time Fourier Transform (DT-FT), Aliasing Problem, Digital Signal Processing (DSP).

* ผู้ประสานงานหลัก (Corresponding Author)
e-mail: Patanavijit@yahoo.com

Mathematical Tutorial of Discrete-Time Analysis of Aliasing and Non-Aliasing Periodic Sampling Concept with Fourier Analysis for Digital Signal Processing and Digital Communication Prospective

**Acknowledgment

The Research was funded by Assumption University

บทคัดย่อ

เนื่องจากความต้องการในการใช้งานสัญญาณดิจิทัลและสัญญาณที่ไม่ต่อเนื่องเชิงเวลาอย่างเช่น สัญญาณเสียง สัญญาณภาพและสัญญาณข้อมูล มีสูงขึ้นทั้งสำหรับการประยุกต์ใช้งานและการวิจัยใน อุปกรณ์อิเล็กทรอนิกส์ในปัจจุบันอย่างเช่น โทรศัพท์มือถือ เครื่อง PDA หรือกล้องดิจิทัลเป็นต้น แต่เนื่องจาก สัญญาณต้นแบบที่บันทึกได้จะมีลักษณะเป็นสัญญาณที่ต่อเนื่องเชิงเวลา (Continuous-Time) ดังนั้น สัญญาณเหล่านี้จึงต้องถูกแปลงเป็นสัญญาณที่ไม่ต่อเนื่องเชิงเวลา (Discrete-Time) โดยใช้เทคนิคทาง คณิตศาสตร์อย่างเช่นการชักตัวอย่างแบบสม่ำเสมอ (Uniform Sampling) หรือการการชักตัวอย่างแบบ ไม่สม่ำเสมอ (Non-Uniform Sampling) ดังนั้นบทความนี้จะนำเสนอหลักการและแนวคิดเชิงคณิตศาสตร์ ของการวิเคราะห์ของสัญญาณที่ไม่ต่อเนื่องเชิงเวลาซึ่งได้จากระบบการชักตัวอย่างทั้งที่มีปัญหาการเคลือบแฝง (Aliasing Problem) และไม่มีปัญหาการเคลือบแฝง (Non-Aliasing Problem) โดยการวิเคราะห์ทาง คณิตศาสตร์ในโดเมนความถี่ ส่วนแรกของบทความนี้จะกล่าวถึงหลักการทางคณิตศาสตร์ของการชักตัวอย่าง แบบสม่ำเสมอสำหรับสัญญาณต้นแบบที่มีลักษณะเป็นคาบ (Periodic) และในส่วนที่สองจะกล่าวถึง หลักการทางคณิตศาสตร์ของการทำงานของระบบการชักตัวอย่างและสัญญาณที่ผ่านกระบวนการชักตัวอย่าง หลักการทางคณิตศาสตร์ของการทำงานของระบบสร้างคืนสัญญาณต้นแบบที่บันทึกได้ซึ่งจะมีลักษณะเป็น สัญญาณที่ต่อเนื่องเชิงเวลาจากสัญญาณที่ผ่านระบบการชักตัวอย่าง นอกจากนี้แล้วยังได้มีกล่าวถึงทฤษฎี การชักตัวอย่างของไนควิสต์และชานนอน (Nyquist-Shannon Sampling Theorem) ส่วนสุดท้าย ของบทความจะกล่าวถึงตัวอย่างของสัญญาณเมื่อผ่านกระบวนการชักตัวอย่างและการสร้างคืนสัญญาณ โดยจะอธิบายทางคณิตศาสตร์อย่างละเอียดเพื่อให้ผู้อ่านมีความเข้าใจอย่างลึกซึ้งเกี่ยวกับทฤษฎีและหลักการ

คำสำคัญ: การแปลงฟูเรียร์ของสัญญาณต่อเนื่องเชิงเวลา การแปลงฟูเรียร์ของสัญญาณดิสครีต ปัญหา การเคลือบแฝง การประมวลผลสัญญาณดิจิทัล

1. Mathematic of Periodic Sampling Concept

From sampling process with uniform sampling technique (Oppenheim & Schaffer, 2009), a sequence of sampled signal, which is acquired from the continuous-time (CT) original signal $x_c(t)$ [Haykin & Veen, 2003; Oppenheim et al., 1997; Phillips et al., 2007] can be mathematically defined as

$$x[n] = x_c(nT); \quad -\infty < n < \infty, \quad (1)$$

where T is the sampling period therefore the sampling frequency can be mathematically defined as $f_s = 1/T$ (samples per second) or $\Omega_s = 2\pi/T$ (radians per second).

The system of sampling process, which can be mathematically written as the above equation, is usually defined as the ideal continuous-to-discrete-time (C/D) that can be illustrated in the figure 1.

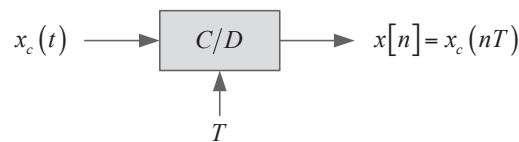


Figure 1 Block diagram of sampling process system (the ideal continuous-to-discrete-time).

From the system property prospective, the sampling system is typically not invertible or noninvertible (so called non-invertible system [Phillips et al., 2007]) because many CT original signals $x_c(t)$ (an input signal) can generate the same sampled signal $x[n]$ (an output signal).

In general, the system of sampling process can be mathematically represented in the two states, which comprises of an impulse train modulator and the sequence generation from the impulse train, as shown in the figure 2.

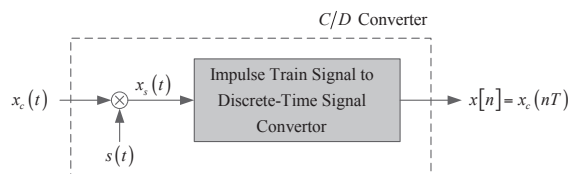


Figure 2 (a) The system of sampling process with periodic impulse train where $x_c(t)$ is the CT original signal, $x_s(t)$ is the result of the impulse train sampling, $x[n]$ is the DT signal.

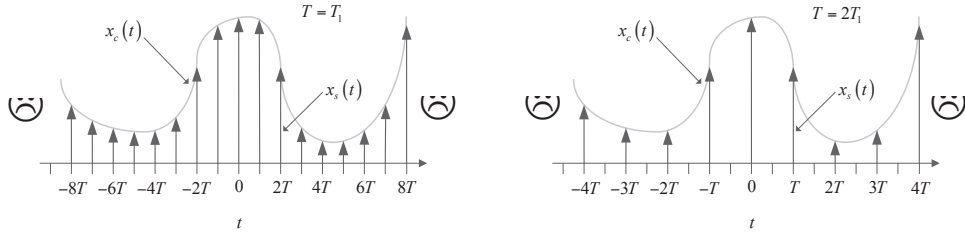


Figure 2 (b) The relationship between $x_c(t)$ (the input signal) and $x_s(t)$ with different sampling rates.

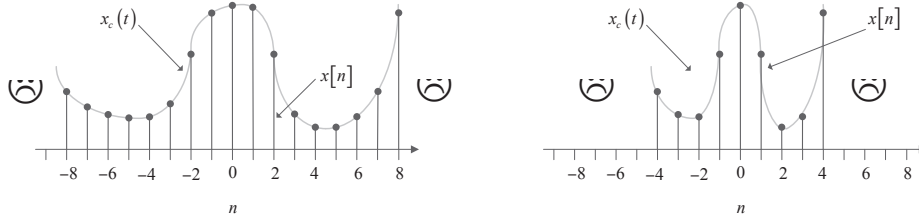


Figure 2 (c) The relationship between $x_c(t)$ (the input signal) and $x[n]$ (the output signal or the DT signal) with different sampling rates.

The periodic impulse train $s(t)$, which is illustrated in Figure 1, can be defined as

$$s(t) = \sum_{n=-\infty}^{\infty} \delta(t - nT) \quad (2)$$

where $\delta(t)$ is the unit impulse (or Dirac delta) function (Wylie & Barrett 1995; Kreyszig, 2011).

The $x_s(t)$ can be mathematically defined as the product of $x_c(t)$ and $s(t)$.

$$x_s(t) = x_c(t)s(t)$$

$$x_s(t) = x_c(t) \sum_{n=-\infty}^{\infty} \delta(t - nT) \quad (3.1)$$

$$x_s(t) = \sum_{n=-\infty}^{\infty} x_c(t) \delta(t - nT) \quad (3.2)$$

Based on the “shifting property” of the continuous-time impulse function, $x(t)\delta(t) = x(0)\delta(t)$ (Wylie & Barrett, 1995; Kreyszig, 2011), $x_s(t)$ can be mathematically written as

$$x_s(t) = \sum_{n=-\infty}^{\infty} x_c(t) \delta(t - nT)$$

$$x_s(t) = \sum_{n=-\infty}^{\infty} x_c(nT) \delta(t - nT) \quad (4)$$

From Eq.(4), the magnitude of the $x_s(t)$ (or the impulse signal at sampled time) is equal to the magnitude of the CT original signals $x_c(t)$ (the input signal) at that sampled time.

The relationship between $x_c(t)$ (the input signal), $x_s(t)$ (the result of the impulse train sampling with different sampling rates and $x[n]$ (the output signal) can be illustrated in Figure 2 (b) and Figure 2 (c). From these figures, the important dissimilar between $x_s(t)$ and $x[n]$ is that the $x_s(t)$ is a CT signal, which is based on an impulse function, and $x[n]$ is a discrete-time (DT) signal.

2. Mathematical Analysis of Sampling System in Frequency Domain

2.1 Mathematical Analysis of Sampling System in Frequency Domain

This section mathematically presents the analysis of sampling system (Oppenheim & Schaffer, 2009; Ingle & Proakis, 2000) in order to demonstrate the relationship between the CT original signal $x_c(t)$, which is usually defined as a band-limited signal as shown in Figure 3(a), and the DT output signal $x[n]$ in frequency domain as shown in Figure 3(c).

The periodic impulse train $s(t)$ can be expressed in the Fourier transform form $S(j\Omega)$ as shown below:

$$s(t) = \sum_{n=-\infty}^{\infty} \delta(t - nT) \xrightarrow{F} S(j\Omega) = \frac{2\pi}{T} \sum_{k=-\infty}^{\infty} \delta(\Omega - k\Omega_s) \quad (5)$$

where $\Omega_s = 2\pi/T$ (radians per second) is the sampling frequency

The $x_s(t)$ or the result of the impulse train sampling can be expressed in the Fourier transform form $X_s(j\Omega)$ as follow:

$$\begin{aligned} x_s(t) = x_c(t) \times s(t) &\xrightarrow{F} X_s(j\Omega) = \frac{1}{2\pi} X_c(j\Omega) * S(j\Omega) \\ X_s(j\Omega) &= \frac{1}{2\pi} X_c(j\Omega) * \left(\frac{2\pi}{T} \sum_{k=-\infty}^{\infty} \delta(\Omega - k\Omega_s) \right) \\ X_s(j\Omega) &= \left(\frac{1}{2\pi} \times \frac{2\pi}{T} \right) \left(X_c(j\Omega) * \sum_{k=-\infty}^{\infty} \delta(\Omega - k\Omega_s) \right) \\ X_s(j\Omega) &= \frac{1}{T} \sum_{k=-\infty}^{\infty} X_c(j(\Omega - k\Omega_s)) \end{aligned} \quad (6)$$

where “*” is the CT convolution operator

In general, the Fourier transform of the result of the impulse train sampling $X_s(j\Omega)$ can be classified into two cases: $\Omega_s \geq 2\Omega_N$ and $\Omega_N \leq \Omega_c \leq (\Omega_s - \Omega_N)$.

For the first case of $X_s(j\Omega) = \frac{1}{T} \sum_{k=-\infty}^{\infty} X_c(j(\Omega - k\Omega_s))$ when $\Omega_s - \Omega_N \geq \Omega_N$ or $\Omega_s \geq 2\Omega_N$, the Fourier transform of the CT original signal $X_c(j\Omega)$, Fourier transform of the periodic impulse train $S(j\Omega)$ and the Fourier transform of the result of the impulse train sampling $X_s(j\Omega)$ can be illustrated as Figures 3(a), 3(b) and 3(c), respectively. From Figure 3(c), the duplication of $X_c(j\Omega)$ does not overlap therefore the accumulation result in $X_s(j\Omega) = \frac{1}{T} \sum_{k=-\infty}^{\infty} X_c(j(\Omega - k\Omega_s))$ clearly demonstrates that there is the multiple duplication form of $X_c(j\Omega)$ as shown in the following figure. As a result, the $X_c(j\Omega)$ can be perfectly reconstructed from $X_s(j\Omega)$ by using the ideal low pass filter (Oppenheim & Schaffer, 2009). (so called non-aliasing distortion or non-aliasing)

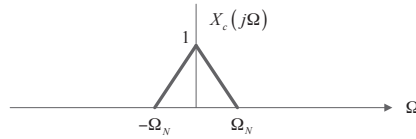


Figure 3 (a) The frequency-domain transform of the CT original signal $x_c(t)$ (the input signal).

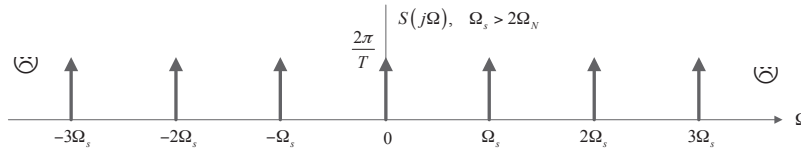


Figure 3 (b) The frequency-domain transform of the periodic impulse train $s(t)$ ($\Omega_s \geq 2\Omega_N$).

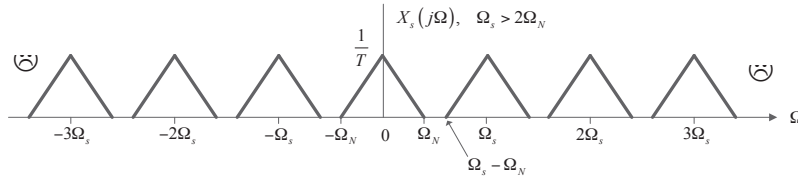


Figure 3 (c) The frequency-domain transform of the result of the impulse train sampling $x_s(t)$.

For the second case of $X_s(j\Omega) = \frac{1}{T} \sum_{k=-\infty}^{\infty} X_c(j(\Omega - k\Omega_s))$ when $\Omega_N \leq \Omega_c \leq (\Omega_s - \Omega_N)$, the Fourier transform of the CT original signal $X_c(j\Omega)$, Fourier transform of the periodic impulse train $S(j\Omega)$ and the Fourier transform of the result of the impulse train sampling $X_s(j\Omega)$ can be illustrated as Figures 4(a), 4(b) and 4(c), respectively. From Figure 4(c), the duplication of $X_c(j\Omega)$ does overlap therefore the accumulation result in $X_s(j\Omega) = \frac{1}{T} \sum_{k=-\infty}^{\infty} X_c(j(\Omega - k\Omega_s))$ demonstrates that there is an unclear and unseparated multiple duplication form of $X_c(j\Omega)$. As a result, the $X_c(j\Omega)$ can be not perfectly reconstructed from $X_s(j\Omega)$ by using the ideal low pass filter (so called aliasing distortion or aliasing).

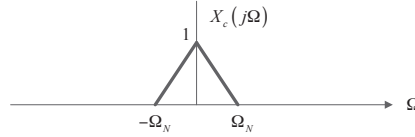


Figure 4 (a) The frequency-domain transform of the CT original signal $x_c(t)$ (the input signal).

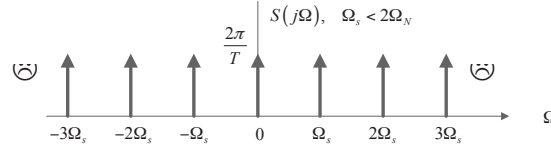


Figure 4 (b) The frequency-domain transform of the periodic impulse train $s(t)$ ($\Omega_N \leq \Omega_c \leq (\Omega_s - \Omega_N)$).

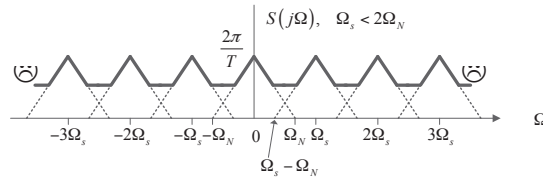


Figure 4 (c) The frequency-domain transform of the result of the impulse train sampling $x_s(t)$.

2.2 Mathematical Analysis of Reconstruction System of the Sampling Signal

For non-aliasing case, the CT original signal $X_c(j\Omega)$ (as shown in Figure 5(a)) can be perfectly reconstructed from the result of the impulse train sampling $X_s(j\Omega)$ (as shown in Figure 5(c)) by using the ideal low pass filter when $\Omega_s - \Omega_N \geq \Omega_N$ or $\Omega_s \geq 2\Omega_N$. Therefore, the relationship among the CT original signal $X_c(j\Omega)$, the result of the impulse train signal $X_s(j\Omega)$, the transfer function of an ideal low pass filter $H_r(j\Omega)$ and the reconstructed signal $X_r(j\Omega)$ are illustrated as shown in Figure 5(a), 5(c), 5(d) and 5(f), respectively.

If the reconstructed signal $X_r(j\Omega)$ (as shown in Figure 5(d)) can be mathematically written as $X_r(j\Omega) = H_r(j\Omega)X_s(j\Omega)$ where this ideal low pass filter has gain T and cutoff frequency Ω_c at $\Omega_N \leq \Omega_c \leq (\Omega_s - \Omega_N)$ then $X_r(j\Omega) = X_c(j\Omega)$ or $x_r(t) = x_c(t)$ (as shown in the Figure 5(a) and 5(f)). However, if $\Omega_s < 2\Omega_N$ (or aliasing case) then the duplication form of $X_c(j\Omega)$ overlap (as shown in the Figure 4(c) in aliasing case) therefore $X_s(j\Omega) = \frac{1}{T} \sum_{k=-\infty}^{\infty} X_c(j(\Omega - k\Omega_s))$ is the unclear and unseparated multiple duplication form of $X_c(j\Omega)$ and $X_c(j\Omega)$ cannot be perfectly reconstructed from $X_s(j\Omega)$ by using an ideal low pass filter.

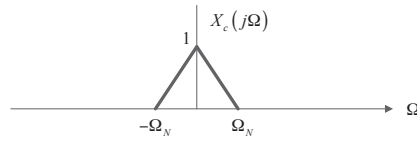


Figure 5 (a) The frequency-domain transform of the CT original signal $x_c(t)$ (the input signal).

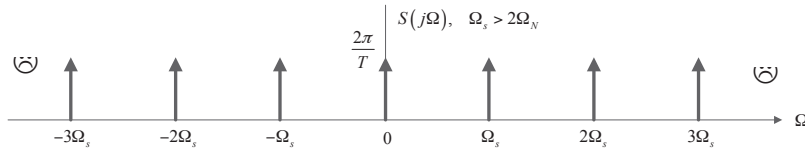


Figure 5 (b) The frequency-domain transform of the result of the impulse train sampling $x_s(t)$.

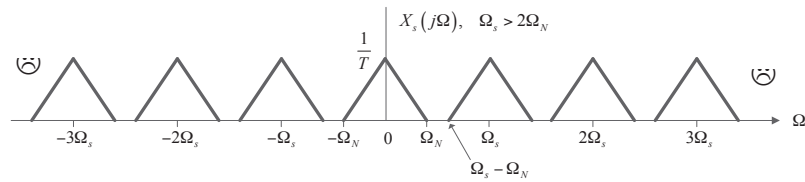


Figure 5 (c) The frequency-domain transform of the result of the impulse train sampling $x_s(t)$.

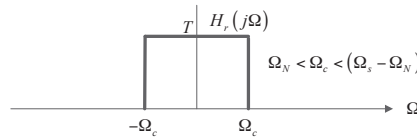


Figure 5 (d) The frequency-domain transform of the ideal lowpass filter.

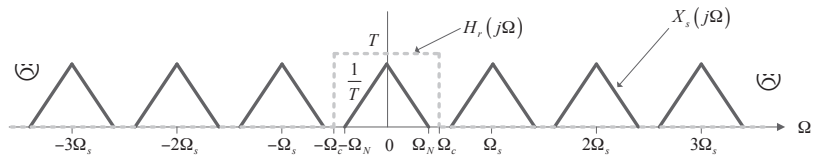


Figure 5 (e) The frequency-domain transform of the ideal lowpass filter process of the result of the impulse train sampling $x_s(t)$.

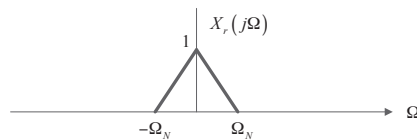


Figure 5 (f) The frequency-domain transform of the result of $x_r(t)$, which is the result of ideal lowpass filter process of the result of the impulse train sampling $x_s(t)$.

2.3 Example of Sampling Signals

For deeply mathematically understanding about both aliasing and non-aliasing cases, this section presents the sampling case of a cosine signal $x_c(t) = \cos(\Omega_0 t)$, as shown in Figure 6(a), in the frequency domain prospective. The Fourier transform of a cosine signal, as shown in Figure 6(b), can be mathematically written as following equation.

$$x_c(t) = \cos(\Omega_0 t) \xrightarrow{F} X_c(j\Omega) = \pi\delta(\Omega - \Omega_0) + \pi\delta(\Omega + \Omega_0) \quad (7)$$

First, for non-aliasing case ($\Omega_s \geq 2\Omega_N$), the relationship between the CT original signal $X_c(j\Omega) = \pi\delta(\Omega - \Omega_0) + \pi\delta(\Omega + \Omega_0)$ (as shown in Figure 6(b)), the result of the impulse train signal $X_s(j\Omega)$ (as shown in Figure 6(d)), the transfer function of an ideal low pass filter $H_r(j\Omega)$ (as shown in Figure 6(d)) and the reconstructed signal $X_r(j\Omega)$ (as shown in Figure 6(e)) can be illustrated as Figure 6. Consequently, the reconstructed signal $X_r(j\Omega) = \pi\delta(\Omega - \Omega_0) + \pi\delta(\Omega + \Omega_0)$ (as shown in Figure 6(e)) or $x_r(t) = \cos(\Omega_0 t)$ ($x_r(t) = x_c(t)$) (as shown in Figure 6(e)) can be perfectly recovered by using an ideal low pass filter $H_r(j\Omega)$.

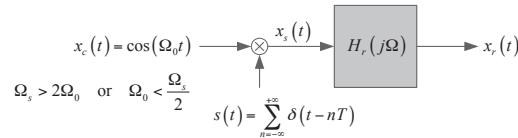


Figure 6 (a) The block diagram of conversion between CT original signal $x_c(t) = \cos(\Omega_0 t)$, the sampled signal $x_s(t)$ and the reconstructed signal $x_r(t)$ in frequency-domain transform.

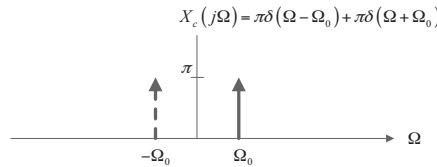


Figure 6 (b) The frequency-domain transform of the CT original signal $x_c(t) = \cos(\Omega_0 t)$.

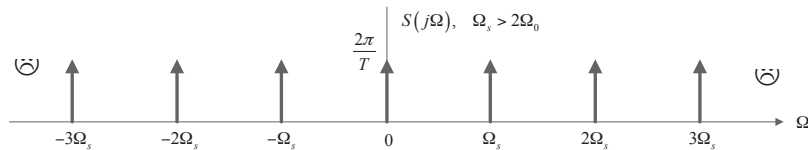


Figure 6 (c) The frequency-domain transform of the result of the impulse train sampling $x_s(t)$ ($\Omega_s \geq 2\Omega_N$).

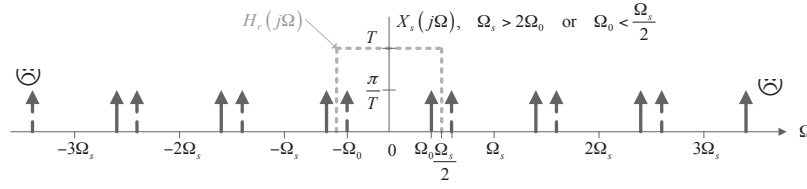


Figure 6 (d) The frequency-domain transform of the ideal lowpass filter process of the result of the impulse train sampling $x_s(t)$ ($\Omega_s \geq 2\Omega_N$).

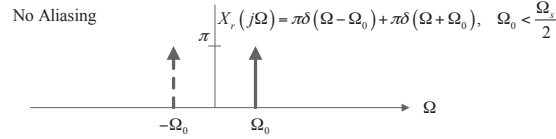


Figure 6 (e) The frequency-domain transform of the result of $x_r(t)$, which is the result of ideal lowpass filter process of the result of the impulse train sampling $x_s(t)$ (Non-Aliasing).

Later, for aliasing case ($\Omega_N \leq \Omega_c \leq (\Omega_s - \Omega_N)$), the relationship between the CT original signal $X_c(j\Omega) = \pi\delta(\Omega - \Omega_0) + \pi\delta(\Omega + \Omega_0)$ (as shown in Figure 7(b)), the result of the impulse train signal $X_s(j\Omega)$ (as shown in Figure 7(d), the transfer function of an ideal low pass filter $H_r(j\Omega)$ (as shown in Figure 7(d) and the reconstructed signal $X_r(j\Omega)$ (as shown in Figure 7(e) can be illustrated as figure 7. Consequently, the reconstructed signal $X_r(j\Omega) = \pi\delta(\Omega - (\Omega_s - \Omega_0)) + \pi\delta(\Omega + (\Omega_s - \Omega_0))$ (as shown in Figure 7(e) or $x_r(t) = \cos((\Omega_s - \Omega_0)t)$, which is not identical with $x_c(t) = \cos(\Omega_0 t)$ (as shown in Figure 7(b)), cannot be perfectly recovered from $X_s(j\Omega)$ by using an ideal low pass filter $H_r(j\Omega)$.

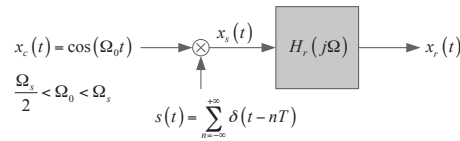


Figure 7 (a) The block diagram of conversion between CT original signal $x_c(t) = \cos(\Omega_0 t)$, the sampled signal $x_s(t)$ and the reconstructed signal $x_r(t)$ in frequency-domain transform.

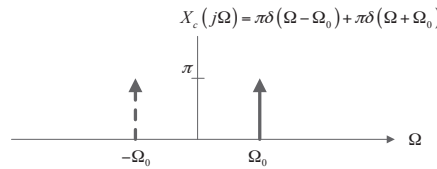


Figure 7 (b) The frequency-domain transform of the CT original signal $x_c(t) = \cos(\Omega_0 t)$.

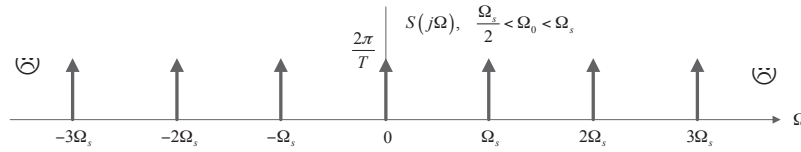


Figure 7 (c) The frequency-domain transform of the result of the impulse train sampling $x_s(t)$ ($\Omega_N \leq \Omega_c \leq (\Omega_s - \Omega_N)$).

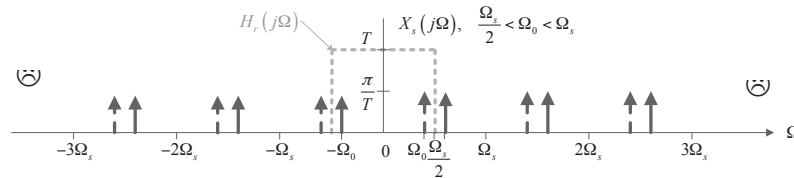


Figure 7 (d) The frequency-domain transform of the ideal lowpass filter process of the result of the impulse train sampling $x_s(t)$ ($\Omega_N \leq \Omega_c \leq (\Omega_s - \Omega_N)$).

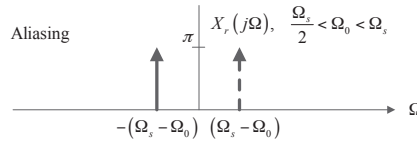


Figure 7 (e) The frequency-domain transform of the result of $x_r(t) \neq x_c(t)$, which is the result of ideal lowpass filter process of the result of the impulse train sampling $x_s(t)$.

2.4 Nyquist-Shannon Sampling Theorem

The sampling case of both aliasing and non-aliasing, which is discussed in the previous section, is the basic ideal of the Nyquist-Shannon theorem as follow.

If a CT original signal $x_c(t)$ is defined as a bandlimited signal ($X_c(j\Omega) = 0$ for $|\Omega| \geq \Omega_N$) and if the sampling frequency is greater than or equal to a double of a maximum frequency of that bandlimited signal or $\Omega_s = \frac{2\pi}{T} \geq 2\Omega_N$ then $x_c(t)$ can be perfectly reconstructed by its sampled signal $x[n]$ where $x[n] = x_c(nT)$, $n = 0, \pm 1, \pm 2, \dots$. In general, the frequency Ω_N is usually defined as the Nyquist frequency and $2\Omega_N$ is usually defined as the Nyquist rate.

The CT Fourier transform of the result of the impulse train sampling $X_s(j\Omega)$ can be mathematically written as following equation.

$$x_s(t) = \sum_{n=-\infty}^{\infty} x_c(nT) \delta(t - nT) \xrightarrow{F} X_s(j\Omega) = \frac{1}{T} \sum_{n=-\infty}^{\infty} x_c(nT) e^{-j\Omega nT} \quad (8)$$

From $x[n] = x_c(nT)$, the CT Fourier transform of the result of the impulse train sampling $X_s(j\Omega)$ can be mathematically simplified as following equation.

$$\begin{aligned} X_s(j\Omega) &= \frac{1}{T} \sum_{n=-\infty}^{\infty} x_c(nT) e^{-j\Omega T n} \\ X(e^{j\omega}) &= \sum_{n=-\infty}^{\infty} x[n] e^{-j\omega n} \end{aligned} \quad (9)$$

Due to $X_s(j\Omega) = X(e^{j\omega}) \Big|_{\omega=\Omega T} = X(e^{j\Omega T})$ and $X_s(j\Omega) = \frac{1}{T} \sum_{k=-\infty}^{\infty} X_c(j(\Omega - k\Omega_s))$, $X(e^{j\Omega T})$ can

be mathematically simplified as following equation.

$$\begin{aligned} X(e^{j\Omega T}) &= X_s(j\Omega) \\ X(e^{j\Omega T}) &= \frac{1}{T} \sum_{k=-\infty}^{\infty} X_c(j(\Omega - k\Omega_s)) \\ X(e^{j\omega}) &= \frac{1}{T} \sum_{k=-\infty}^{\infty} X_c\left(j\left(\frac{\omega}{T} - \frac{2\pi k}{T}\right)\right) \end{aligned} \quad (10)$$

The term $X(e^{j\omega})$ is the DT-Fourier Transform and is the frequency scaling of $X_s(j\Omega)$ with $\omega = \Omega T$.

For time-domain prospective, the sampled signal $x[n]$ always has the unity spacing where the sampling period is set to be T or the sampling frequency is set to be $f_s = 1/T$.

3. Example of Sampling and Reconstruction

3.1 Example of Sampling and Reconstruction of Non-Aliasing Case ($\Omega_s \geq 2\Omega_N$)

If the CT original signal $x_c(t) = \cos(4000\pi t)$ and the sampling period is $T = 1/6000$ then the sampled signal $x[n] = x_c(nT) = \cos(4000\pi T n) = \cos(\omega_0 n)$ with $\omega_0 = 4000nT = 2\pi/3$. Consequently, sampling frequency $\Omega_s = 2\pi/T = 12000\pi$ and the highest frequency of the CT original signal $x_c(t)$ is $\Omega_0 = 4000\pi$ therefore Nyquist sampling theorem is fulfilled $\Omega_s \geq 2\Omega_N$ ($\Omega_s = 12000\pi$ and $\Omega_N = 4000\pi$). The Fourier transform of the CT original signal $x_c(t) = \cos(4000\pi t)$ can be mathematically written as following equation.

$$x_c(t) = \cos(4000\pi t) \xrightarrow{F} X_c(j\Omega) = \pi\delta(\Omega - 4000\pi) + \pi\delta(\Omega + 4000\pi) \quad (11)$$

And the result of the impulse train signal $X_s(j\Omega)$ can be mathematically written as following equation.

$$X_s(j\Omega) = \frac{1}{T} \sum_{k=-\infty}^{\infty} X_c(j(\Omega - k\Omega_s)) \text{ for } \Omega_s = 12000\pi. \quad (12)$$

From the above equation (as shown in Figure 8(a)), the CT original signal $X_c(j\Omega)$ is a pair of impulses at $\Omega = \pm 4000\pi$ and the result of the impulse train signal $X_s(j\Omega)$ is the shifted copies of the pair of impulses ($X_c(j\Omega)$) (as shown in Figure 8(a)), which is centered on $\pm\Omega_s, \pm 2\Omega_s$, ect. where $\Omega_s = 12000\pi$.

By using the DTFT, $X(e^{j\omega}) = X_s(j\omega/T)$ with $\omega = \Omega T$ as shown in Figure 8(b) and the highest frequency of the CT original signal $x_c(t)$ is $\Omega_0 = 4000\pi$ correlates to the normalized frequency $\omega_0 = 4000\pi T = 2\pi/3$, which is fulfilled the Nyquist sampling theorem or $\Omega_s \geq 2\Omega_0$ ($\Omega_s = 12000\pi$ and $\Omega_0 = 4000\pi$). Consequently, this sampling case is non-aliasing case and the CT original signal $X_c(j\Omega)$ (as shown in Figure 8(c)) can be perfectly recovered from $X_s(j\Omega)$ by using an ideal low pass filter $H_r(j\Omega)$ as shown in these Figures 8(a)-8(c).

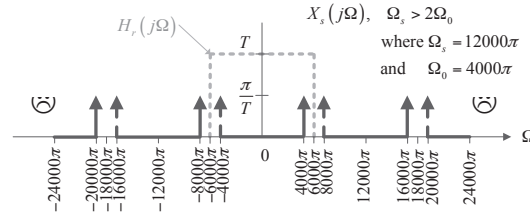


Figure 8(a) The frequency-domain transform (based on CT-FT) of the ideal lowpass filter process of the result of the impulse train sampling $x_s(t)$ ($\Omega_s = 12000\pi$ and $\Omega_0 = 4000\pi$).

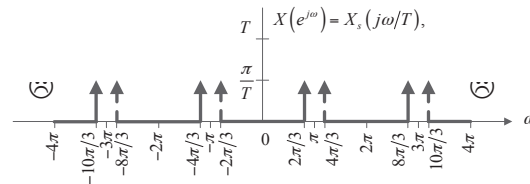


Figure 8(b) The frequency-domain transform (based on DT-FT) of the result of the impulse train sampling $x_s(t)$ ($\Omega_s = 12000\pi$ and $\Omega_0 = 4000\pi$).

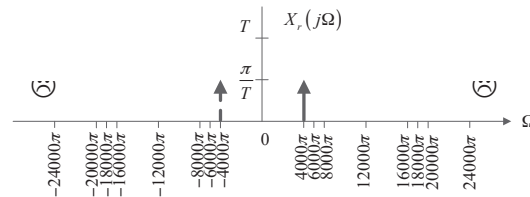


Figure 8(c) The frequency-domain transform of the result of $x_r(t) = x_c(t) = \cos(4000\pi t)$, which is the result of ideal lowpass filter process of the result of the impulse train sampling $x_s(t)$ (Non-Aliasing).

3.2 Example of Sampling and Reconstruction of Aliasing Case ($\Omega_s < 2\Omega_N$)

If the CT original signal $x_c(t) = \cos(16000\pi t)$ and the sampling period is $T = 1/6000$ then the sampled signal $x[n] = x_c(nT) = \cos(16000\pi Tn)$ or $x[n] = x_c(nT) = \cos(\omega_0 n)$ with $\omega_0 = 16000nT = 8\pi/3 = 2\pi + 2\pi/3$. Consequently, sampling frequency $\Omega_s = 2\pi/T = 12000\pi$ and the highest frequency of the CT original signal $x_c(t)$ is $\Omega_0 = 16000\pi$ therefore Nyquist sampling theorem is not fulfilled $\Omega_s < 2\Omega_N$ ($\Omega_s = 12000\pi$ and $\Omega_N = 16000\pi$). The Fourier transform of the CT original signal $x_c(t) = \cos(16000\pi t)$ can be mathematically written as following equation.

$$x_c(t) = \cos(16000\pi t) \xrightarrow{F} X_c(j\Omega) = \pi\delta(\Omega - 16000\pi) + \pi\delta(\Omega + 16000\pi) \quad (13)$$

And the result of the impulse train signal $X_s(j\Omega)$ can be mathematically written as following equation.

$$X_s(j\Omega) = \frac{1}{T} \sum_{k=-\infty}^{\infty} X_c(j(\Omega - k\Omega_s)) \text{ for } \Omega_s = 12000\pi \quad (14)$$

From this above equation (as shown in Figure 9(b)), the CT original signal $X_c(j\Omega)$ is a pair of impulses at $\Omega = \pm 16000\pi$ and the result of the impulse train signal $X_s(j\Omega)$ is the shifted copies of the pair of impulses ($X_c(j\Omega)$), which is centered on $\pm\Omega_s, \pm 2\Omega_s$, ect. where $\Omega_s = 12000\pi$. Consequently, the result of the impulse train signal $X_s(j\Omega)$ (as shown in the Figure 9(a-b)) is identical to the $X_s(j\Omega)$ from the previous case ($x_c(t) = \cos(4000\pi t)$) (as shown in the Figure 8(a)) and the sampling period is $T = 1/6000$ therefore CT reconstructed signal $X_r(j\Omega)$, which is reconstructed from $X_s(j\Omega)$ by using an ideal low pass filter $H_r(j\Omega)$ is $X_r(j\Omega) = \pi\delta(\Omega - 4000\pi) + \pi\delta(\Omega + 4000\pi)$ (as shown in Figure 9(c)) or $x_r(t) = \cos(4000\pi t)$ and this result is not equal to the CT original signal $x_c(t) = \cos(16000\pi t)$ (this case is so called the aliasing problem). From this result, the the CT original signal $x_c(t) = \cos(16000\pi t)$ cannot be reconstructed by using the result of the impulse train signal $X_s(j\Omega)$ where $\Omega_s = 12000\pi$ because the Nyquist sampling theorem is not fulfilled or $\Omega_s < 2\Omega_N$.

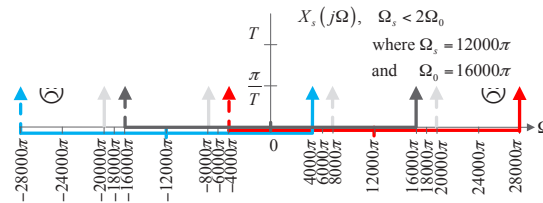


Figure 9 (a) The frequency-domain transform (based on CT-FT) of the ideal low pass filter process of the result of the impulse train sampling $x_s(t)$ ($\Omega_s = 12000\pi$ and $\Omega_0 = 16000\pi$).

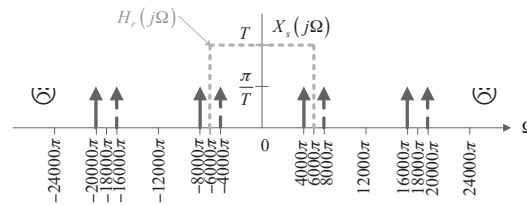


Figure 9 (b) The frequency-domain transform (based on DT-FT) of the result of the impulse train sampling $x_s(t)$ ($\Omega_s = 12000\pi$ and $\Omega_0 = 16000\pi$).

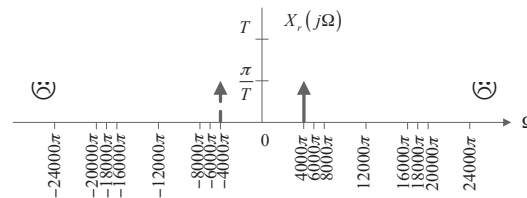


Figure 9 (c) The frequency-domain transform of the result of $x_r(t) \neq x_c(t) = \cos(16000\pi t)$, which is the result of ideal low pass filter process of the result of the impulse train sampling $x_s(t)$ (Aliasing).

4. Conclusion

The primary objectives of this paper were to contribute aliasing and non-aliasing periodic sampling concepts and their mathematical background for researching advanced algorithms or mathematical techniques. Therefore, this paper describes the periodic sampling concept, the frequency domain mathematical analysis in sampling result, reconstruction result and the Nyquist-Shannon sampling theorem, aliasing and non-aliasing sampling concepts and an example of the sampling process and reconstruction process. The sampling theory is one of the most crucial mathematical topics in the DT signal/system research field during this decade. Hence, a lot of mathematical explanations and figures were provided in this paper.

Furthermore, authors have also applied the aliasing and non-aliasing periodic sampling concepts in the research field of the Super Resolution Reconstruction (SRR) (Patanavijit, 2011; Patanavijit, 2016) for reconstructing the higher resolution signal by using Aliasing periodic sampled signal.

References

- Haykin, S. & Veen, B. V. (2003). *Signals and Systems*. John Wiley & Sons, Inc., 2nd Edition.
- Ingle, V. K. & Proakis, J. G. (2000), *Digital Signal Processing using Matlab*, Brooks/Cole Thomson Learning.
- Kreyszig, E. (2011). *Advanced Engineering Mathematics*. John Wiley & Sons, Inc., 10th Edition.
- Oppenheim, A.V. & Schaffer, R.W. (2009). *Discrete-Time Signal Processing*. Prentice Hall, 3rd Edition.
- Oppenheim, A. V., Willsky, A. S. & Nawab, S. H. (1997). *Signals and Systems*. Prentice-Hall, 2nd Edition.
- Phillips, L., Parr, J. M. & Riskin, E. A. (2007). *Signals, Systems, and Transforms*. Prentice-Hall, 4th Edition.

- Patanavijit, V. (2011). The empirical performance study of a super resolution reconstruction based on frequency domain from aliased multi-low resolution images. *In Proceedings of The 34th Electrical Engineering Conference (EECON-34), Ambassador City Jomtien Hotel, Pataya, Chonburi, Thailand, Dec.*, pp. 645-648.
- Patanavijit, V. (2016). Conceptual framework of super resolution reconstruction based on frequency domain from Aliased multi-low resolution images: theory part. *Panyapiwat Journal*, 8(2), 284-297.
- Wylie, C. R. & Barrett, L. C. (1995). *Advanced Engineering Mathematics*. McGraw-Hill Companies, Inc., 6th Edition.

Authors

Asst. Prof. Dr.Vorapoj Patanavijit

Vincent Mary School of Engineering (VME Building 2nd floor)
 Assumption University (Suvarnabhumi Campus), 88 Moo 8 Bang Na-Trad Km.26,
 Bangsaothong, Samuthprakarn, Thailand, 10540
 e-mail: patanavijit@yahoo.com

Asst. Prof. Dr.Kornkamol Thakulsukanant

Martin de Tours School of Management and Economics (MSME Building 2nd floor)
 Assumption University (Suvarnabhumi Campus), 88 Moo 8 Bang Na-Trad Km.26,
 Bangsaothong, Samuthprakarn, Thailand, 10540
 e-mail: kthakulsukanant@yahoo.com

